

# Neutron Star Masses and Radii

J. M. Lattimer

Department of Physics & Astronomy



Xiamen-CUSTIPEN Workshop on the EOS of Dense Neutron-rich Matter  
in the Era of Gravitational Wave Astronomy  
Xiamen, China  
3–7 January, 2019

# Neutron Star Mass and Radius Measurements

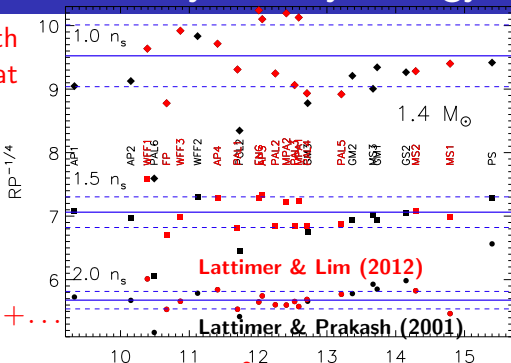
- ▶ Constraints from GR, causality and the neutron star maximum mass
- ▶ Theoretical and experimental constraints from nuclear physics
- ▶ Photospheric radius expansion bursts
- ▶ Quiescent low-mass X-ray binaries
- ▶ Pulsar timing
- ▶ NICER and moment of inertia constraints
- ▶ Tidal deformabilities and GW170817

# Neutron Star Radii and Nuclear Symmetry Energy

- ▶ Radii are highly correlated with neutron star matter pressure at  $1 - 2n_s \simeq 0.16 - 0.32 \text{ fm}^{-3}$ .
- ▶ Neutron star matter is nearly pure neutrons,  $x \sim 0.04$ .
- ▶ Nuclear symmetry energy

$$S(n) \equiv E_0(n) - E_{1/2}(n)$$

$$E_x(n) \simeq E_{1/2}(n) + S_2(n)(1-2x)^2 + \dots$$



$$S(n) \simeq S_2(n) \simeq S_v + \frac{L}{3} \frac{n - n_s}{n_s} + \frac{K_{sym}}{18} \left( \frac{n - n_s}{n_s} \right)^2 \dots$$

- ▶  $S_v \equiv S_2(n_s) \sim 32 \text{ MeV}$ ,  $L \sim 50 \text{ MeV}$ ; nuclear systematics.
- ▶ Neutron matter energy and pressure at  $n_s$ :

$$E_0(n_s) \simeq S_v + E_{1/2}(n_s) = S_v - B \sim 13 - 17 \text{ MeV}$$

$$p_0(n_s) = \left( n^2 \frac{\partial E_0(n)}{\partial n} \right)_{n_s} \simeq \frac{L n_s}{3} \sim 2.1 - 3.7 \text{ MeV fm}^{-3}$$

# Causality + GR Limits and the Maximum Mass

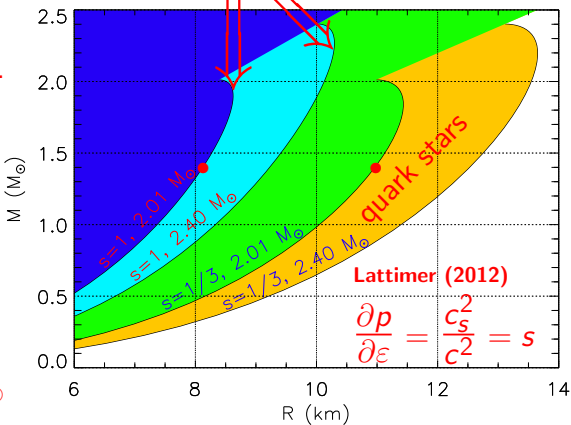
A lower limit to the maximum mass sets a lower limit to the radius for a given mass.

Similarly, a precision upper limit to  $R$  sets an upper limit to the maximum mass.

$R_{1.4} > 8.15$  (10.9) km  
if  $M_{max} \geq 2.01 M_{\odot}$ .

$M_{max} < 3.93$  (2.52)  $M_{\odot}$   
if  $R < 13$  km.

$M - R$  curves for maximally compact EOS



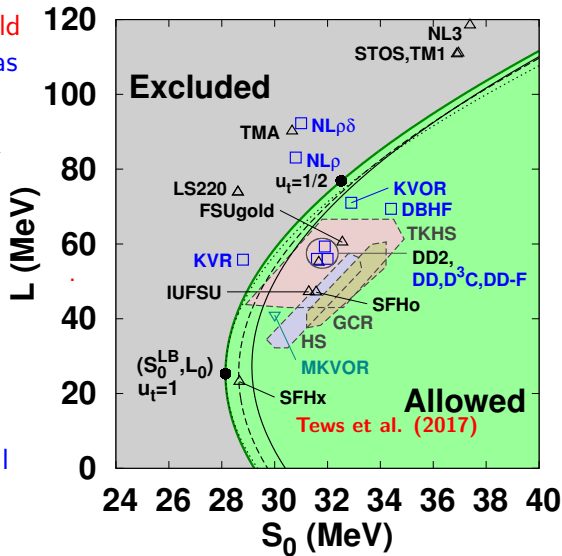
If quark matter exists in the interior, the minimum radii are substantially larger; maximum masses are considerably smaller.

# Unitary Gas Bounds

Neutron matter energy should be larger than the unitary gas energy  $E_{UG} = \xi_0(3/5)E_F$

$$E_{UG} = 12.6 \left( \frac{n}{n_s} \right)^{2/3} \text{ MeV}$$

The unitary gas refers to fermions interacting via a pairwise short-range s-wave interaction with an infinite scattering length and zero range. Cold atom experiments show a universal behavior with the Bertsch parameter  $\xi_0 \simeq 0.37$ .



$$S_v \geq 28.6 \text{ MeV}; L \geq 25.3 \text{ MeV}; \rho_0(n_s) \geq 1.35 \text{ MeV fm}^{-3}; R_{1.4} \geq 9.7 \text{ km}$$

# Theoretical and Experimental Constraints

H Chiral Lagrangian

G: Quantum Monte Carlo

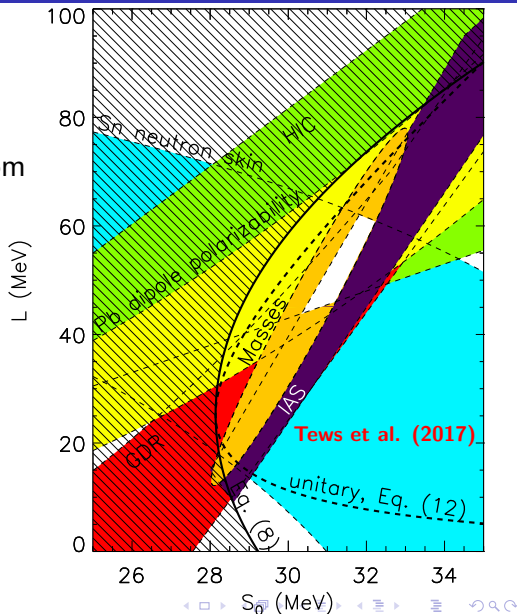
neutron matter calculations from  
Hebeler et al. (2012)

unitary gas constraints from

Combined experimental  
constraints are compatible  
with unitary gas bounds.

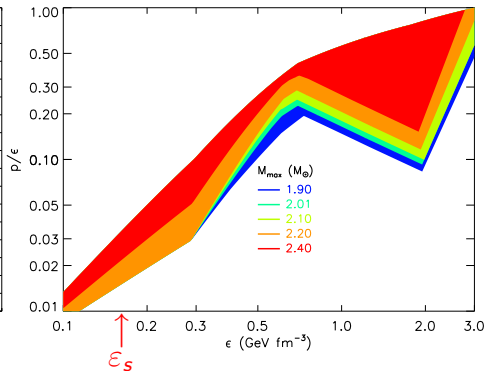
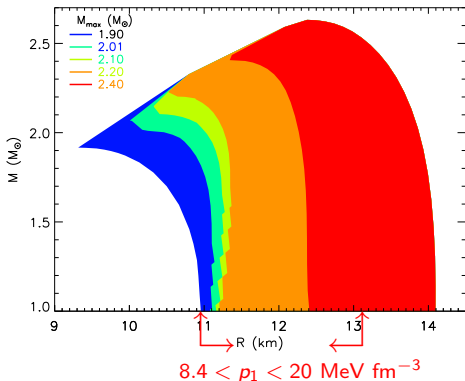
Neutron matter calculations  
are compatible with both.

$$10.9 \text{ km} \leq R_{1.4} \leq 13.1 \text{ km}$$



# Predictions Using Piecewise Polytopes

Both the assumed minimum value of the neutron star maximum mass and the assumed matter pressure at  $n_1 = 1.5 - 2n_s$  are important in restricting  $M - R$  and  $p - \epsilon$  values.



Zhao & Lattimer (2018)

# Simultaneous Mass and Radius Measurements

- ▶ Measurements of flux  $F_\infty = (R_\infty/D)^2 \sigma T_{\text{eff}}^4$  and color temperature  $T_c \propto \lambda_{\text{max}}^{-1}$  yield an apparent angular size (pseudo-BB):

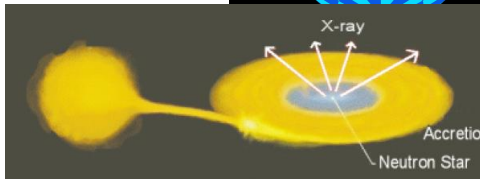
$$R_\infty/D = (R/D) / \sqrt{1 - 2GM/Rc^2}$$

- ▶ Observational uncertainties include distance  $D$ , nonuniform  $T$ , interstellar absorption  $N_H$ , atmospheric composition

Best chances are:

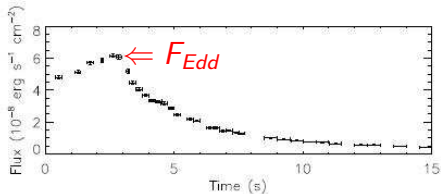
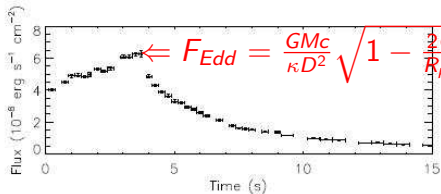
- ▶ Isolated neutron stars with parallax (atmosphere ??)
- ▶ Quiescent low-mass X-ray binaries (QLMXBs) in globular clusters (reliable distances, low  $B$  H-atmospheres)
- ▶ Bursting sources with peak fluxes close to Eddington limit (PREs); gravity balances radiation pressure

$$F_{\text{Edd}} = \frac{cGM}{\kappa D^2} \sqrt{1 - 2GM/Rc^2}$$

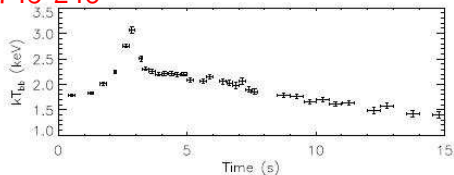
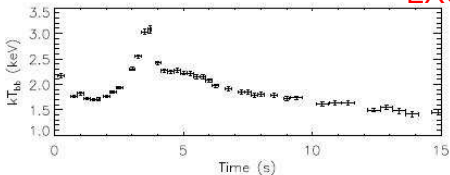




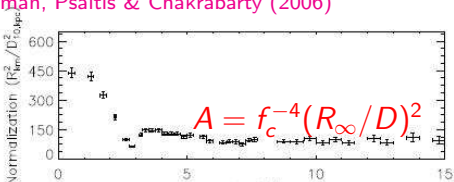
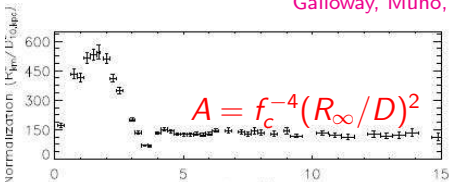
# Photospheric Radius Expansion X-Ray Bursts



EXO 1745-248



Galloway, Muno, Hartman, Psaltis & Chakrabarty (2006)



# PRE Burst Models

Ozel et al.  $z_{\text{ph}} = z$   $\beta = GM/Rc^2$

Steiner et al.  $z_{\text{ph}} \ll z$

$$F_{\text{Edd}} = \frac{GMc}{\kappa D} \sqrt{1-2\beta}$$

$$F_{\text{Edd}} = \frac{GMc}{\kappa D}$$

$$A = \frac{F_{\infty}}{\sigma T_{\infty}^4} = f_c^{-4} \left( \frac{R_{\infty}}{D} \right)^2$$

$$\alpha = \beta \sqrt{1-2\beta}$$

$$\theta = \cos^{-1}(1-54\alpha^2)$$

$$\alpha = \frac{F_{\text{Edd}}}{\sqrt{A}} \frac{\kappa D}{F_c^2 c^3} = \beta(1-2\beta)$$

$$\beta = \frac{1}{6} \left[ 1 + \sqrt{3} \sin\left(\frac{\theta}{3}\right) \right.$$

$$\gamma = \frac{A f_c^4 c^3}{\kappa F_{\text{Edd}}} = \frac{R_{\infty}}{\alpha}$$

$$\left. - \cos\left(\frac{\theta}{3}\right) \right]$$

$$\beta = \frac{1}{4} \pm \frac{1}{4} \sqrt{1-8\alpha}$$

$$\alpha \leq \frac{1}{8} \text{ required.}$$

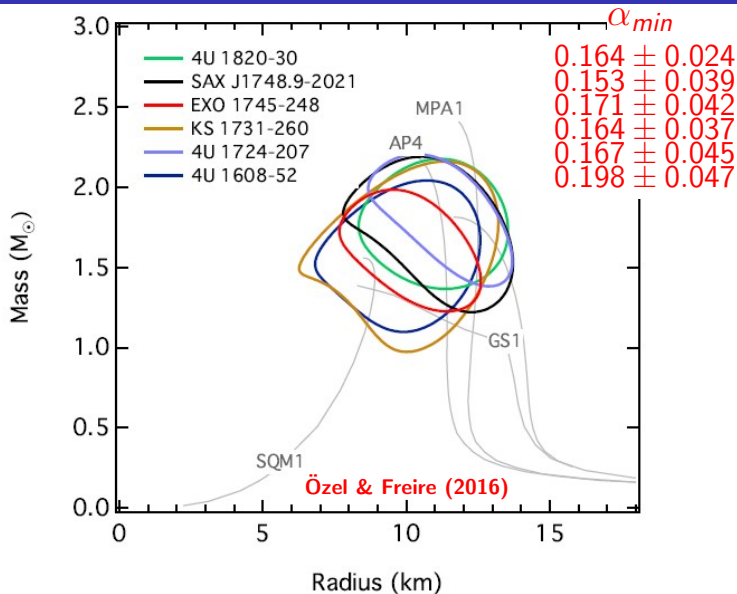
$$\alpha \leq \sqrt{\frac{1}{27}} \simeq 0.192 \text{ required.}$$

EXO1745-248 4U1608-522 4U1820-30 KS1731-260 SAXJ1748.9-2021

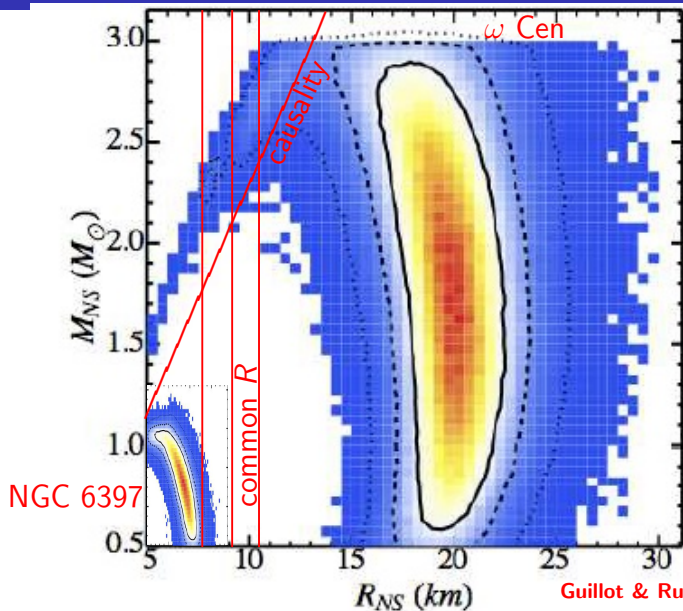
$0.19 \pm 0.04$   $0.25 \pm 0.06$   $0.24 \pm 0.04$   $0.20 \pm 0.03$   $0.18 \pm 0.04$

observed  $\alpha$  values (Ozel et al.)

# PRE $M - R$ Estimates



# QLMXBs

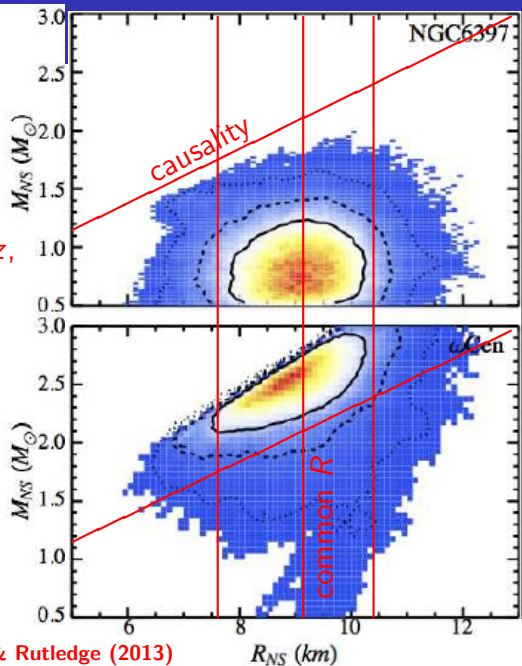


Guillot & Rutledge (2013)

# QLMXBs

Forcing a common radius among sources having disparate values of  $R_\infty$ , with little information concerning their redshifts  $z$ , produces a solution near the smallest  $R_\infty$ .

Sources are then predicted to have widely different radii and masses.



Guillot & Rutledge (2013)

# QLMXB $M - R$ Estimates

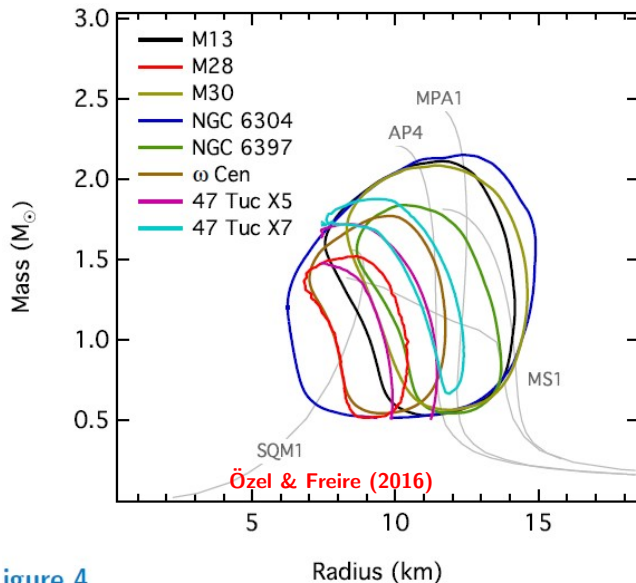
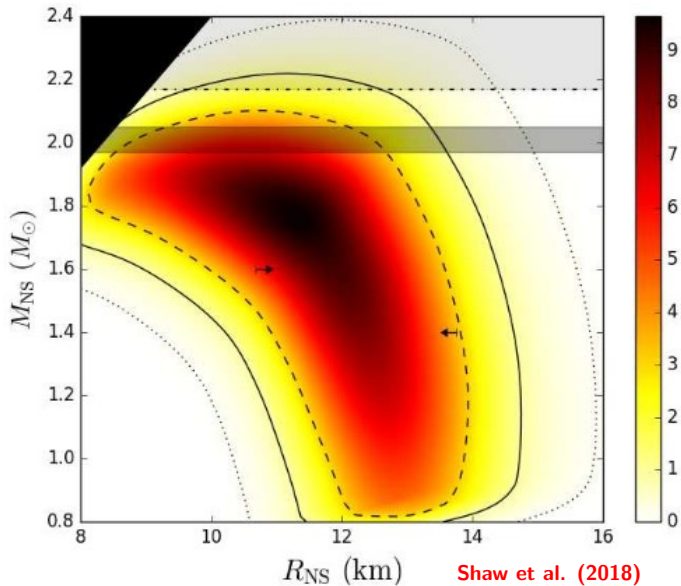


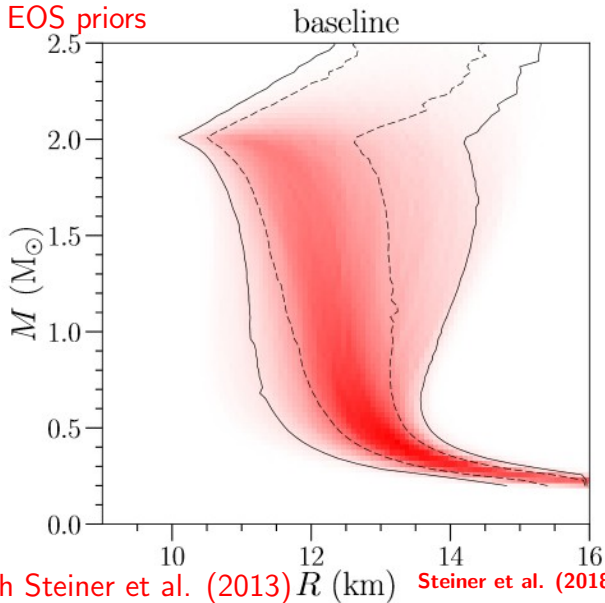
Figure 4

# M13 QLMXB

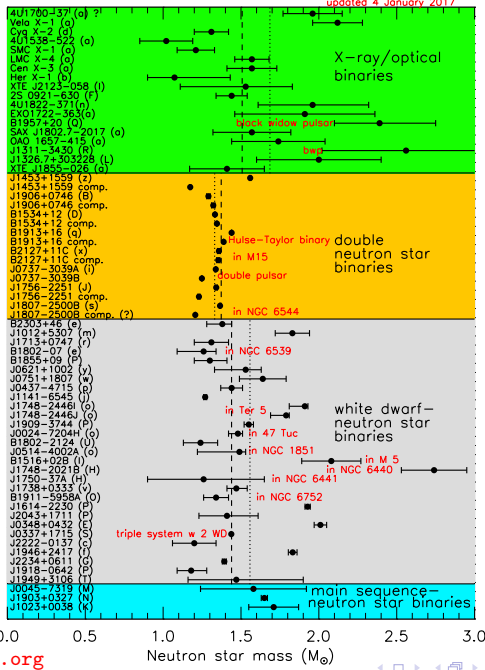


# 8 QLMXBs

Parameterized EOS priors







vanKerkwijk 2010  
Romani et al. 2012

Although simple average mass of w.d. companions is 0.23  $M_{\odot}$  larger, weighted average is 0.04  $M_{\odot}$  smaller

Demorest et al. 2010  
Fonseca et al. 2016  
Antoniadis et al. 2013  
Barr et al. 2016

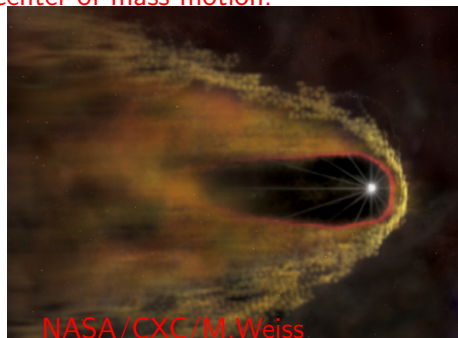
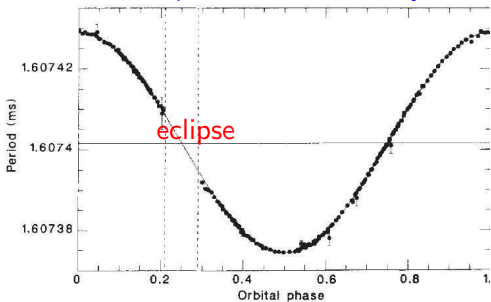
Champion et al. 2008

Lattimer (2012) [stellarcollapse.org](http://www.stellarcollapse.org)

# Black Widow Pulsar PSR B1957+20

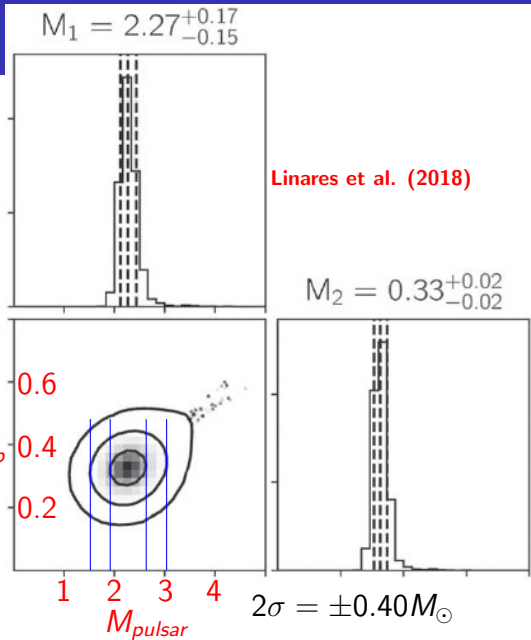
A 1.6ms pulsar in circular 9.17h orbit with  $\sim 0.03 M_{\odot}$  companion. The pulsar is eclipsed for 50-60 minutes each orbit; eclipsing object has a volume much larger than the secondary or its Roche lobe. Pulsar is ablating the companion leading to mass loss and the eclipsing plasma. The secondary may nearly fill its Roche lobe. Ablation by the pulsar leads to secondary's eventual disappearance. The optical light curve tracks the motion of the secondary's irradiated hot spot rather than its center of mass motion.

pulsar radial velocity

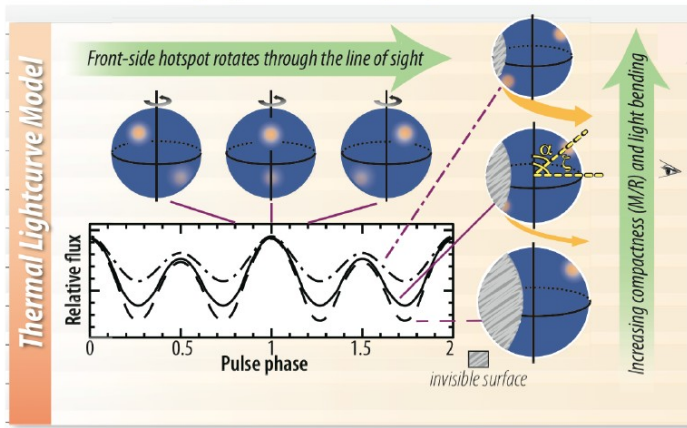


# PSR J2215-5135

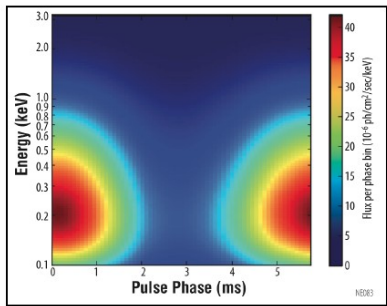
- ▶ Redback binary MSP
- ▶  $P_{orb} = 4.14$  hr
- ▶  $T_{night} = 5660^{+260}_{-380}$  K
- ▶  $T_{day} = 8080^{+470}_{-280}$  K
- ▶  $D = 2.9 \pm 0.1$  kpc
- ▶  $e = 0.144 \pm 0.002$   $M_{comp}$
- ▶ Roche lobe filling factor  $f = 0.95 \pm 0.01$
- ▶  $M_{pulsar} = 2.27^{+0.17}_{-0.15} M_{\odot}$
- ▶  $M_{comp} = 0.33^{+0.02}_{-0.02} M_{\odot}$



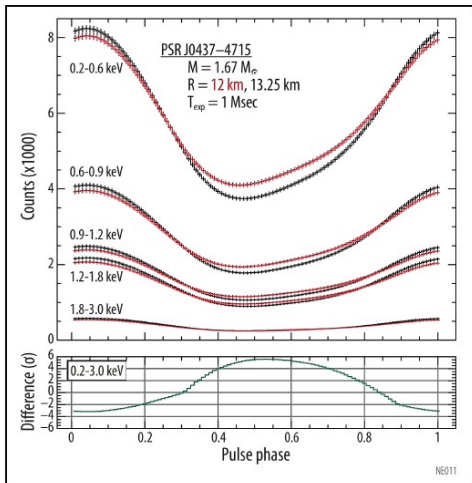
Reveal stellar structure through lightcurve modeling, long-term timing, and pulsation searches



**Lightcurve modeling** constrains the compactness ( $M/R$ ) and viewing geometry of a non-accreting millisecond pulsar through the depth of modulation and harmonic content of emission from rotating hot-spots, thanks to **gravitational light-bending**...

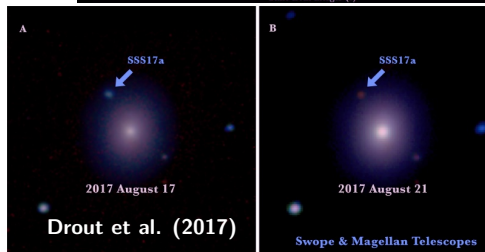
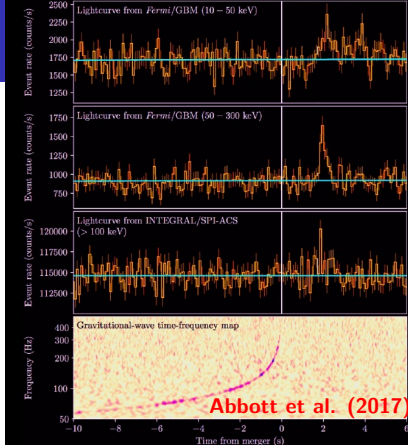


... while phase-resolved spectroscopy promises a direct constraint of radius  $R$ .



# GW170817

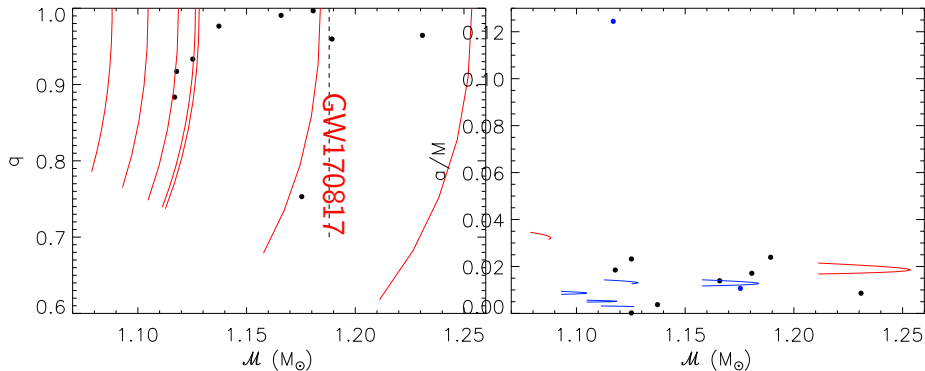
- ▶ LIGO-Virgo detected a signal consistent with a BNS merger, followed 1.7 s later by a weak sGRB.
- ▶ 16600 orbits observed over 165 s.
- ▶  $\mathcal{M}_{\text{chirp}} = 1.1867 \pm 0.0001 M_{\odot}$
- ▶  $M_{\text{tot,max}} = 2^{6/5} \mathcal{M}_{\text{chirp}} = 2.726 M_{\odot}$
- ▶  $E_{\text{rad}} > 0.025 M_{\odot} c^2$
- ▶  $D_L = 40 \pm 10$  Mpc
- ▶  $84 < \tilde{\Lambda} < 640$  (90%)
- ▶  $M_{\text{ejecta}} \sim 0.06 \pm 0.02 M_{\odot}$
- ▶ Blue ejecta:  $\sim 0.01 M_{\odot}$
- ▶ Red ejecta:  $\sim 0.05 M_{\odot}$
- ▶ Likely r-process production



# Properties of Double Neutron Star Binaries

DNS with only an upper limit to  $m_p$

DNS with  $\tau_{GW} = \infty$



# Waveform Model Parameter Determinations

There are 13 free wave-form parameters including finite-size effects at third PN order  $(v/c)^6$ . LV17 used a 13-parameter model; De et al. (2018) used a 9-parameter model.

- ▶ Sky location (2) EM data
  - ▶ Distance (1) EM data
  - ▶ Inclination (1)
  - ▶ Coalescence time (1)
  - ▶ Coalescence phase (1)
  - ▶ Polarization (1)
- } Extrinsic
- ▶ Component masses (2)
  - ▶ Perpendicular spins (2)
  - ▶ Tidal deformabilities (2)  
correlated with masses
- } Intrinsic



# Tidal Deformability

Tidal deformability  $\lambda$  is the ratio between the induced dipole moment  $Q_{ij}$  and the external tidal field  $E_{ij}$ ,  $Q_{ij} \equiv -\lambda E_{ij}$ .

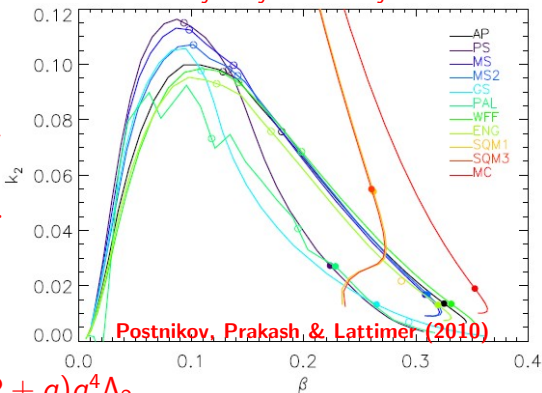
$k_2$  is the dimensionless Love number. It is convenient to work with the dimensionless quantity

$$\Lambda = \frac{\lambda c^{10}}{G^4 M^5} \equiv \frac{2}{3} k_2 \left( \frac{Rc^2}{GM} \right)^5.$$

For a binary neutron star, the relevant quantity is

$$\bar{\Lambda} = \frac{16(1+12q)\Lambda_1 + (12+q)q^4\Lambda_2}{13(1+q)^5}, \quad q = M_2/M_1 \leq 1$$

$$\delta\Phi_t = -\frac{117}{256} \frac{(1+q)^4}{q^2} \left( \frac{\pi f_{GW} GM}{c^3} \right)^{5/3} \bar{\Lambda} + \dots$$



# Deformability and the Radius

▶  $\Lambda = a(Rc^2/GM)^6$

$a = 0.0085 \pm 0.0010$  for

$M = 1.35 \pm 0.25 M_{\odot}$

$$\tilde{\Lambda} = \frac{16(1+12q)\Lambda_1 + q^4(12+q)\Lambda_2}{13(1+q)^5} \Lambda \beta^6$$

▶  $R_1 \simeq R_2 \simeq \hat{R}$

$$\tilde{\Lambda} \simeq \frac{16a}{13} \left( \frac{\hat{R}c^2}{GM} \right)^6 \frac{q^{8/5}(12-11q+12q^2)}{(1+q)^{26/5}}$$

▶  $\tilde{\Lambda} = a'(\hat{R}c^2/GM)^6$

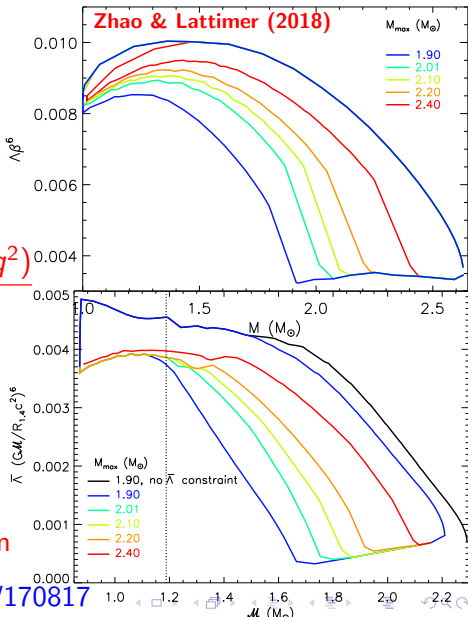
$a' = 0.0035 \pm 0.0007$  for

$\mathcal{M} = 1.2 \pm 0.2 M_{\odot}$

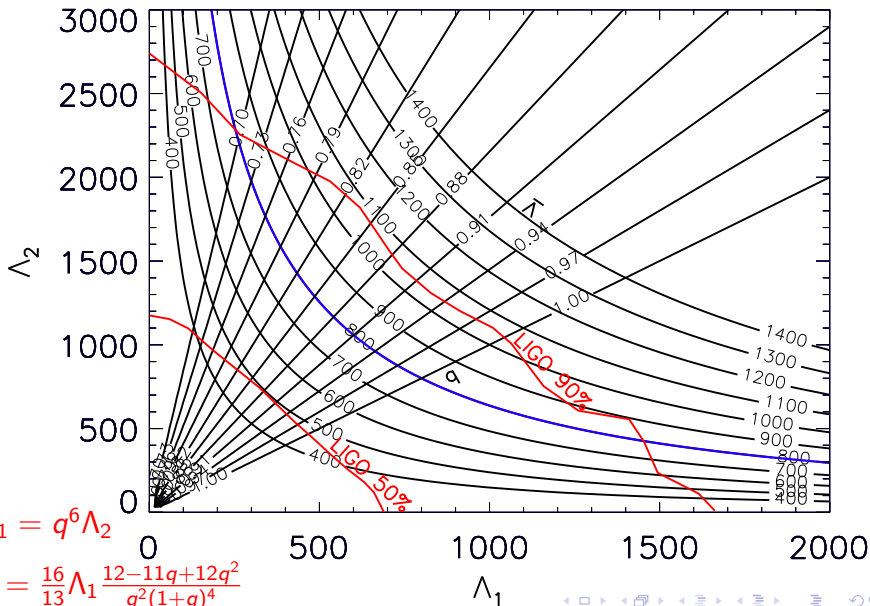
$a' = 0.0039 \pm 0.0002$  GW10817

▶  $\hat{R} = 11.5 \pm 0.3 \frac{\mathcal{M}}{M_{\odot}} \left( \frac{\tilde{\Lambda}}{800} \right)^{1/6} \text{ km}$

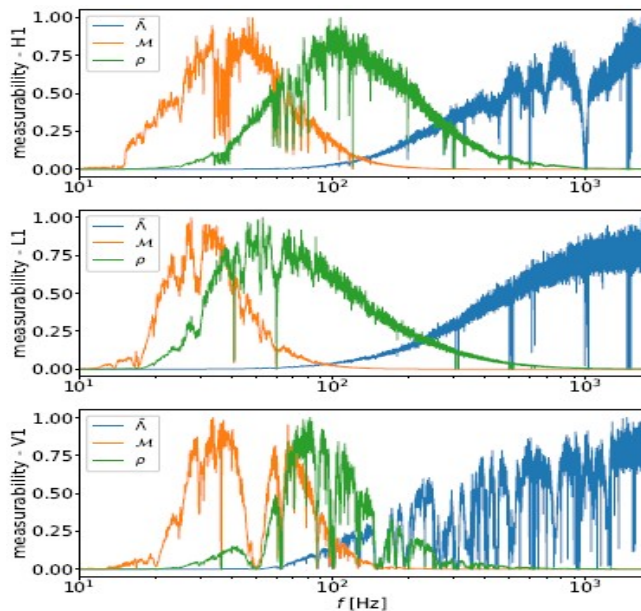
$\hat{R} = 13.4 \pm 0.1 (\tilde{\Lambda}/800)^{1/6} \text{ km}$  GW170817



# Tidal Deformabilities



# Measurability of Tidal Deformability

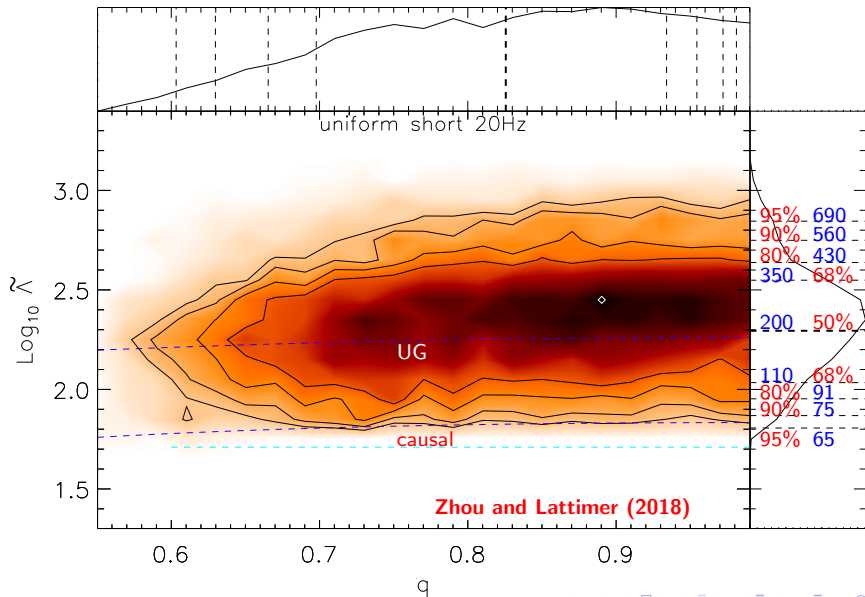


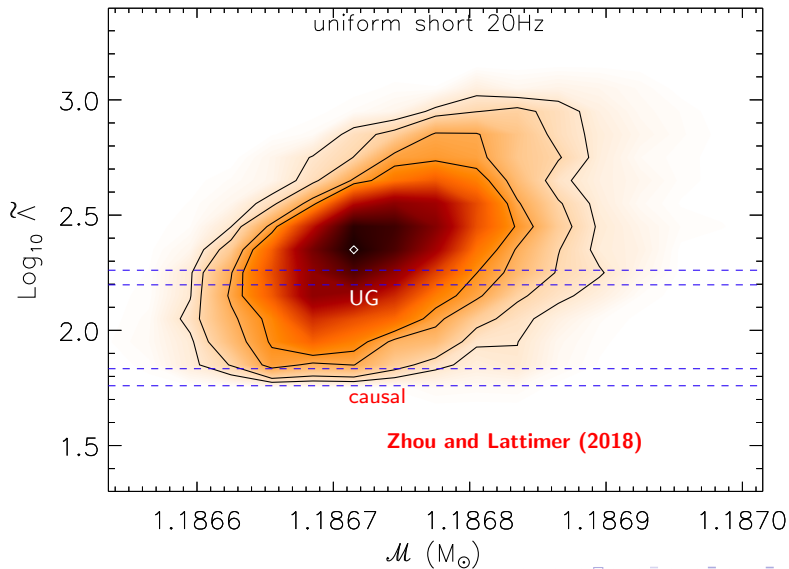
De et al. (2018)

# A Re-Analysis of GW170817 ( De et al. 2018)

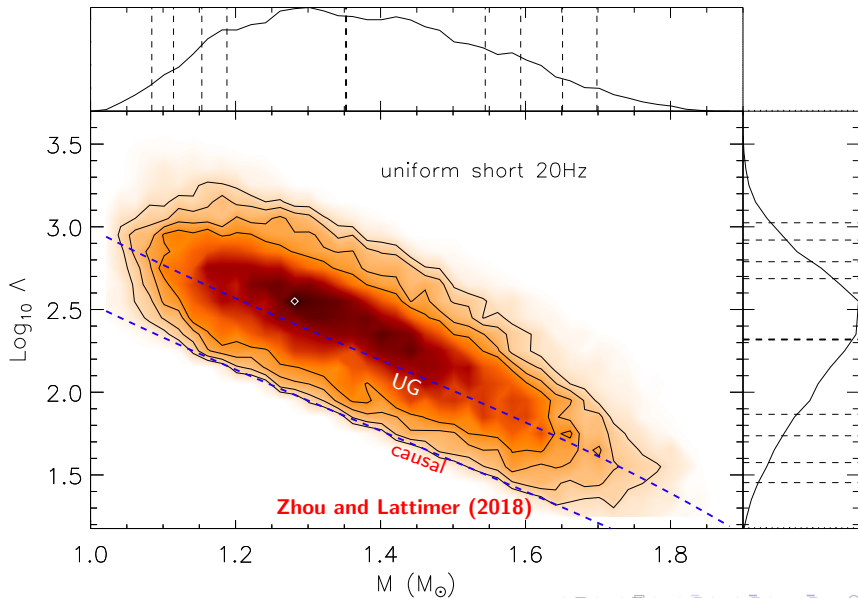
- ▶ De18 takes advantage of the precisely-known electromagnetic source position (Soares-Santos et al., 2017).
- ▶ Uses existing knowledge of the  $H_0$  and the redshift of NGC 4993 to fix the distance (Cantiello et al., 2017).
- ▶ Assumes both neutron stars have the same equation of state, which implies  $\Lambda_1 \simeq q^6 \Lambda_2$ .
- ▶ Baseline model effectively has 9 instead of 13 parameters.
- ▶ Explores variations of mass, spin and deformability priors.
- ▶ Low-frequency cutoff taken to be 20 Hz, not 30 Hz (LV17), doubling the number of analyzed orbits.
- ▶ De18 finds mild evidence ( $\mathcal{B} \sim 10$ ) for finite-size effects, but no evidence for spins.
- ▶ Finds a 90% lower confidence bound to  $\tilde{\Lambda}$ .
- ▶ Finds strong evidence ( $\mathcal{B} \sim 400$ ) for a common EOS, which argues against one star being a hybrid star.
- ▶ Finds including  $\Lambda - M$  correlations reduces  $\tilde{\Lambda}$  by  $\sim 30\%$

# GW170817



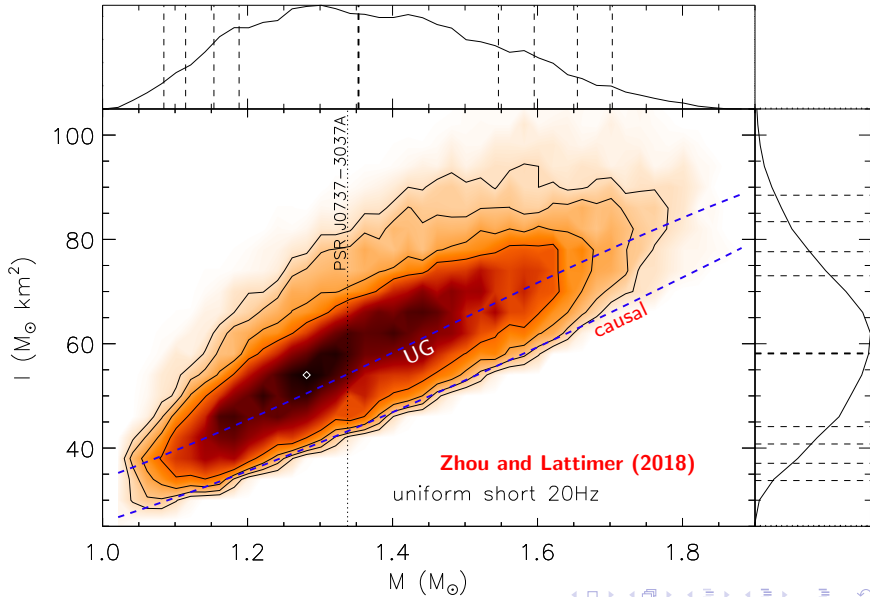


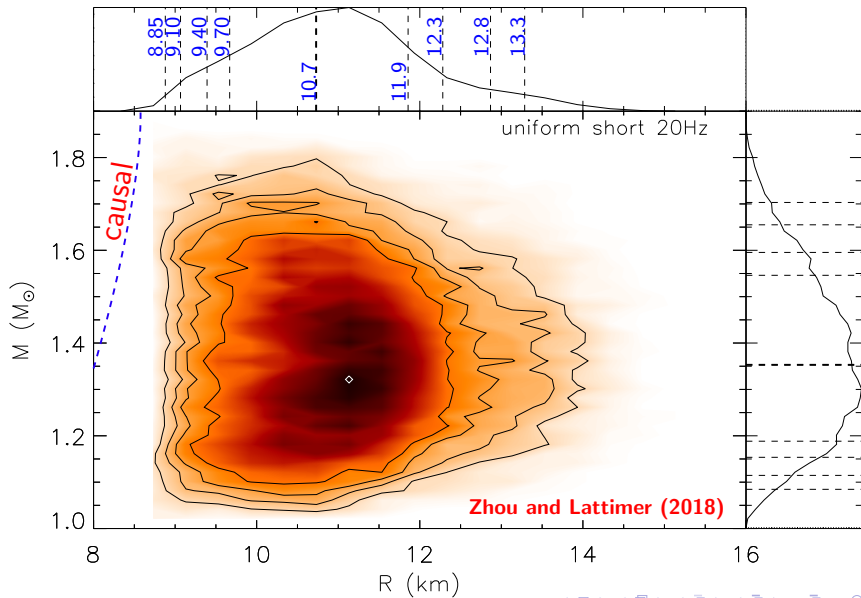
# GW170817





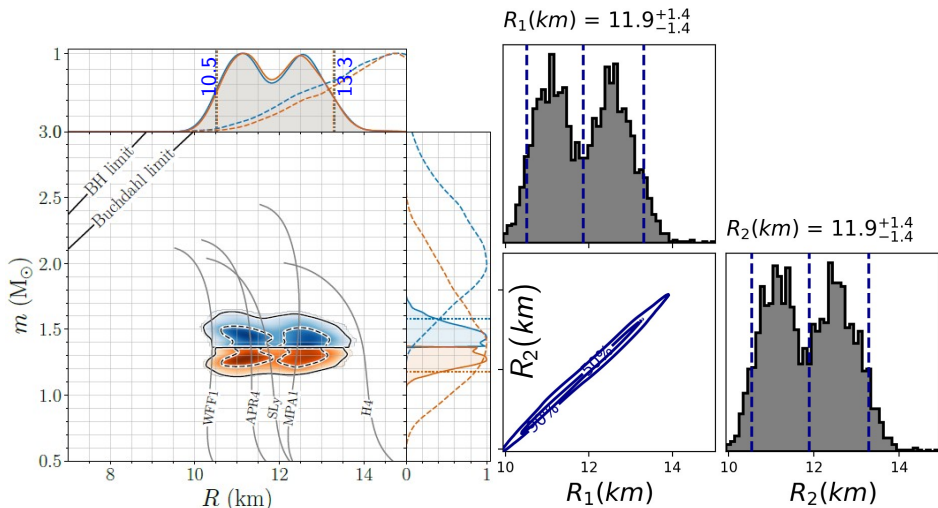
# GW170817





# LV18 Determined $R_1 \simeq R_2$ for GW170817

$\Lambda_2 - \Lambda_1$  correlations from parameterized EOSs with  $M_{max} > 1.97M_\odot$



LV18



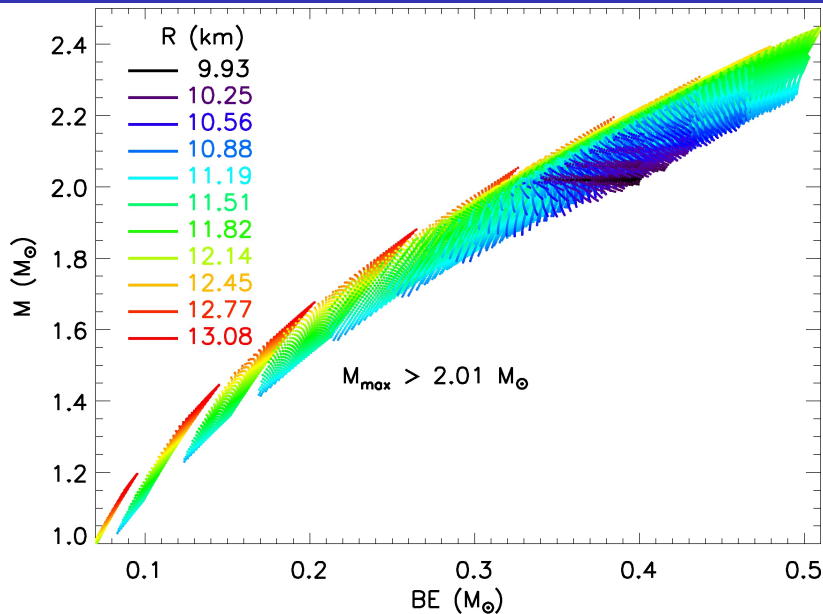
# GW170817 Summary

- ▶ It's important to include correlations among  $\Lambda_1, \Lambda_2, M_1$  and  $M_2$  in a model-independent fashion.
- ▶ It's important to include as many orbits as possible; low frequency cutoff is about 20 Hz.
- ▶ Better waveform models appear to reduce fitting uncertainties in  $\tilde{\Lambda}$  (by about 15%).
- ▶ LV18 constraints on radii depend on how the EOS is modeled. Compared to using bounds on the deformability-mass correlation, their method biases results towards central values of the EOS parameter and radius ranges.
- ▶ Upper bounds to  $M_{max}$  should not play a role in radius determinations, but do in the LV18 analyses.
- ▶ With a better waveform model, De et al. should obtain a 90% confidence upper limit to  $\hat{R}$  of about 12.4 km.
- ▶ With unitary gas constraint,  $\tilde{\Lambda} > 160, \hat{R} > 10.7$  km.
- ▶ Coughlin et al. (2018) claim  $\tilde{\Lambda} > 197$  from EM evidence.

# The Future

- ▶ A few more neutron star mergers per year should allow significant improvements to radii and maximum mass constraints. The systems are expected to be quite similar to GW170817, except they will be further away and may not have optical transients or sGRBs.
- ▶ It should be possible to establish a pulsar-timing bounds to the moment of inertia of PSR 0737-3037A, which with its known mass, will set tight radius constraints.
- ▶ NICER expects to release radius estimates with 1 km-accuracy by years' end.
- ▶ Ongoing and planned nuclear experiments, including neutron skin measurements at J-Lab and Mainz, will offer competing information.
- ▶ Further *ab-initio* improvements will be important.
- ▶ Further measurements of black widow pulsar systems should give us some surprises.

# Binding Energy - Mass Correlations



# Binding Energy - Compactness Correlations

